Experimental study of millimeter wave radiation from a rotating electron beam in a rippled magnetic field

W. W. Destler, F. M. Aghamir, and D. A. Boyd
University of Maryland, College Park, Maryland 20742

G. Bekefi, R. E. Shefer, and Y. Z. Yin[a)]
Massachusetts Institute of Technology, Cambridge, Massachusetts 02139

(Received 18 October 1984; accepted 10 March 1985)

The generation of millimeter wave radiation from the interaction of a rotating electron beam (2 MeV, 1 kA, 5 nsec) with an azimuthally periodic wiggler magnetic field has been studied experimentally. Calculations of the effects of the wiggler magnetic field on the single particle electron orbits are presented, together with experimental measurements of the effects of the wiggler field on the electron beam. Narrow-band radiation at power levels in excess of 200 kW has been observed at 88 and 175 GHz for wiggler fields with 6.28 and 3.14 cm periods, respectively. The radiation frequency spectra for various experimental configurations are presented, and results are compared with theoretical expectations.

I. INTRODUCTION

In recent years many theoretical and experimental studies have been reported of linear free-electron lasers (FEL's) in which short-wavelength radiation is produced by the interaction of an electron beam with a spatially periodic wiggler magnetic field.[1-10] Recently, a novel circular geometry FEL has been explored both theoretically and experimentally in a collaborative effort by researchers at the Massachusetts Institute of Technology and the University of Maryland.[11-16] In this concept, a rotating, relativistic electron beam interacts with an azimuthally periodic wiggler field produced by samarium cobalt magnets placed interior and exterior to the beam. The potential advantages of such systems include a longer effective interaction region, a more compact geometrical configuration, and internal feedback resulting from the recirculation of the electromagnetic wave. This last feature may mean that the device can operate as an oscillator rather than an amplifier, as in the case of linear FEL's.

In the experiments to date, two principal methods have been used to generate the rotating electron beam. The first experiments employed a diode configuration similar to those used in relativistic magnetrons.[11,14] Here the electrons perform $\mathbf{E}\times\mathbf{B}$ drifts around the aximuth in the presence of a radial electric field and an axial magnetic field. Addition of an aximuthally periodic magnetic field then results in a circular FEL. Although initial experimental results from this configuration are encouraging, one potential drawback of this configuration is the considerable electron velocity shear inherent to cross field electron flow in magnetron-like devices.

Recently we published a preliminary study of a second configuration that effectively circumvents this velocity shear problem.[15] This experiment involves the generation of an essentially monoenergetic rotating electron beam by passing a hollow, nonrotating electron beam through a narrow magnetic cusp. In this manner, the $\mathbf{v}_z\times\mathbf{B}_r$ force at the center of the cusp effectively converts the axial beam velocity into rotational velocity downstream of the cusp transition region. If the cusp is symmetric, the downstream beam performs simple axis encircling cyclotron orbits with a gyroradius equal to the radius of the beam on the upstream side of the cusp.[17]

To the axial magnetic field about which the beam electrons rotate is added an azimuthally periodic wiggler field, which is primarily radial near the center of the gap, and thus transverse to the electron beam flow. The wiggler field is produced by samarium cobalt magnets placed behind two concentric metal cylinders in such a way that the beam sees only smooth conducting boundaries. The proximity of the conducting walls to the beam also serves to suppress the negative mass instability, which has been used to produce radiation at microwave frequencies in previous studies.[18,19]

In this paper, we present the first detailed measurements of the operational characteristics of this new circular FEL configuration. Measurements of the effect of the wiggler field on the rotating electron beam are presented, as are radiation spectra obtained for a number of wiggler configurations. Section II of this paper contains a discussion of theoretical considerations, and the experiments are presented in Sec. III. Conclusions are drawn in Sec. IV.

II. THEORETICAL DISCUSSION

A. Electron motion in the axial and wiggler magnetic fields

The general configuration used for these studies is detailed in Fig. 1. Downstream of the cusp transition, the electron orbits have axial (v_{z2}) and azimuthal ($v_{\theta 2}$) velocity components given in terms of the upstream axial velocity (v_{z1}) by

$$v_{z1}^2 = v_{z2}^2 + v_{\theta 2}^2 = v_{z2}^2 + r_c^2\Omega_{\parallel}^2,$$

where r_c is the cathode radius and $\Omega_{\parallel} = eB_z/m_0\gamma$ is the relativistic electron-cyclotron frequency in the downstream axial magnetic field. Thus, as the magnetic field is raised

[a)] Permanent address: Institute of Electronics, Academia Sinica, Beijing, People's Republic of China.

 0031-9171/85/061962-06$01.90

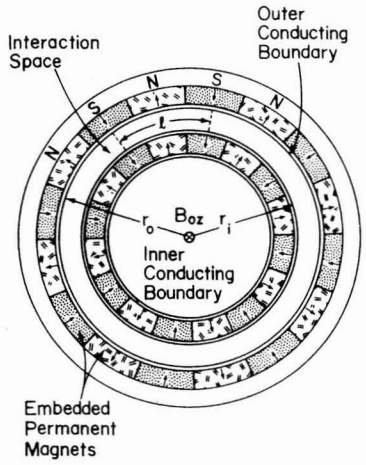

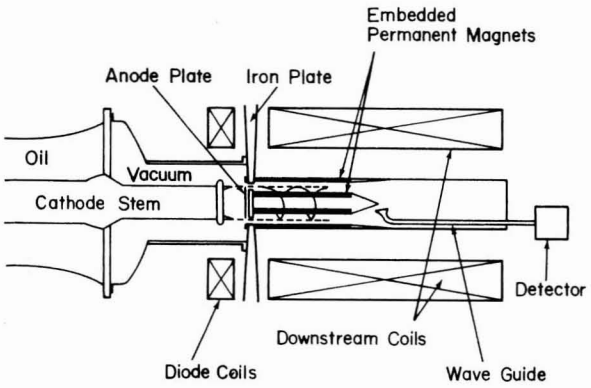

FIG. 1. General experimental configuration.

toward a cutoff value, given by

$$B_{zc} = v_{z1} m_0 \gamma / r_c e,$$

the axial velocity is reduced and electron orbits become fairly tight helices. Beyond the cusp the electrons move in the presence of the combined axial and wiggler magnetic fields, which can be approximated (subject to the condition that $\nabla \cdot \mathbf{B} = \nabla \times \mathbf{B} = 0$ in the region between two conducting boundaries of radii r_0 and r_i) by the expression

$$\mathbf{B} = \hat{r} \frac{B_{0w}}{3} \cos(N\theta) \left[\left(\frac{r}{r_0} \right)^{N-1} + \left(\frac{r_i}{r} \right)^{N+1} \right] \times \left(\frac{r_0}{r_i} \right)^{(N^2-1)/2N} - \hat{\theta} \frac{B_{0w}}{2} \sin(N\theta) \left[\left(\frac{r}{r_0} \right)^{N-1} - \left(\frac{r_i}{r} \right)^{N+1} \right] \left(\frac{r_0}{r_i} \right)^{(N^2-1)/2N} + \hat{z} B_z .$$

Here $\hat{r}$, $\hat{\theta}$, and $\hat{z}$ are unit vectors in the radial, azimuthal, and axial directions, respectively, $N = \pi(r_0 + r_i)/l_0$ is the number of spatial periods around the azimuth, l_0 is the linear periodicity specified midway in the gap, and B_{0w} is the amplitude of the radial component of the field at a distance

$$r = (r_0^{N-1} r_i^{N+1})^{1/(2N)},$$

where the azimuthal component vanishes. It is easily seen that near the center of the gap, the field is primarily radial and that the undulatory $\mathbf{v}_\theta \times \mathbf{B}_r$ force is the $\pm z$ direction, analogous to the transverse motion of electrons in a linear FEL.

Because of the complicated nature of the combined axial and wiggler fields, a single particle computer simulation program has been used to check that the particle orbits are as desired. Figure 2 shows calculated particle orbits with and without the wiggler fields, results that show clearly that the electron orbits are almost unperturbed in the r-θ plane, and the undulation is primarily axial, as desired. While Fig. 2 shows typical electron orbits for an electron with an initial radial position of precisely 6 cm (the cathode radius), electrons launched at other radial positions within the radial width of the beam do not show significantly different behavior. We have performed these calculations for each of the several wiggler field configurations investigated experimentally, and in no case are the electron orbits unsatisfactory.

B. Excitation of TM waves by the rotating electron beam

In a previous theoretical paper by two of the authors (Y. Yin and G. Bekefi),[16] the radiative process has been identified as the coupling of a "synchronous mode,"[20] upshifted in frequency by the wiggler periodicity N:

$$\omega = (l + N)\Omega_{\parallel}$$

to one or more of the TM waves supported by the coaxial conducting boundary system. The radiation frequency is given by

$$\omega = \frac{N\Omega_{\parallel}}{1 - [l\Omega_{\parallel}/\omega_c(l,m)]} = \frac{k_\omega v_\theta}{1 - (v_\theta / v_{p\theta})}$$

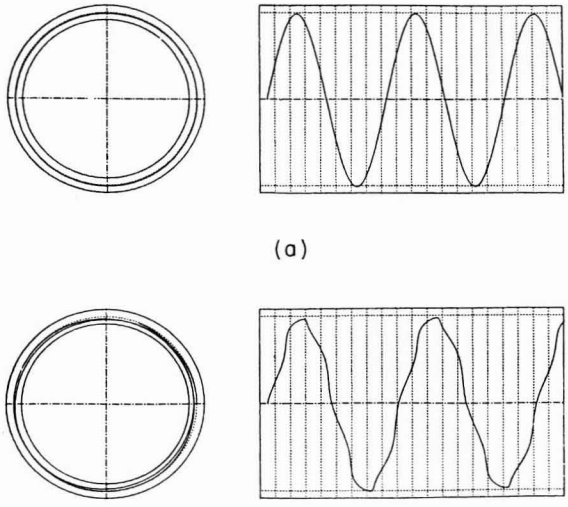

FIG. 2. Calculated particle orbits in the r-θ and r-z planes for an electron injected with $v_z = 0.20c$, $v_\theta = 0.96c$ into the interaction space with (a) $B_z = 1.4$ kG, $B_{0w} = 0$, and (b) $B_z = 1.4$ kG, $B_{0w} = 1.3$ kG.

TABLE I. Computed parameters for an electron ring of radius 6.000 cm rotating in a coaxial waveguide of radii $r_0 = 6.509$ cm, $r_i = 5.398$ cm. $\beta_\theta = 0.968$; $B_{0\omega} = 0.75$ kG; $J_\theta = 1.10$ A cm^{-2}; ω is the radiation frequency; ω_i the temporal growth rate; and η the saturated efficiency.

N	l_0 (cm)	m	l	$\omega/2\pi$ (GHz)	$\omega_i \times 10^{-9}$ (rad sec^{-1})	η (%)
6	6.28	1	29	26.8	1.02	19
6	6.28	1	117	94.7	0.21	0.6
12	3.14	1	7	14.6	0.48	14
12	3.14	1	281	225.6	0.014	0.15
12	3.14	2	56	52.3	0.15	0.83
12	3.14	2	232	187.9	0.031	0.05

where $k_\omega = 2\pi/l_0$, $\omega_c(l,m)$ is the cutoff frequency for the TM_{lm} mode, l and m are the azimuthal and radial wavenumbers, respectively, and

$$v_{p\theta} = \omega_c(l,m)(r/l)$$

is the azimuthal phase velocity of the rf perturbation. It is interesting to compare this result to the dispersion relation for a conventional linear free-electron laser:

$$\omega = \frac{k_\omega v_0}{[1 - (v_0/c)]},$$

where v_0 is now the axial electron velocity.

In the limit where the gap between the two coaxial conducting boundaries is small compared to their mean radius, the cutoff frequency of the TM_{lm} mode may be approximated by the expression

$$\omega_c(l,m) = [m\pi c/r_i(g-1)](1+\alpha l^2)^{1/2},$$

where $g = r_0/r_i$ and

$$\alpha = \left[\frac{2}{m\pi}\left(\frac{g-1}{g+1}\right)\right]^2.$$

The resultant predicted radiation frequencies for actual experimental parameters discussed in the next section are summarized in Table I. For the specified parameters these are the only unstable interactions predicted by the theory. Because these predicted radiation frequencies are quite sensitive to the values chosen for the applied magnetic field and the electron energy, the values indicated in Table I must be treated as estimates. One important conclusion, however, is that high-frequency radiation is predicted for very low values of the radial mode number m, an important result because the electron beam radial width (about 5 mm) is a sizable fraction of the gap between the two coaxial conductors (13 mm). A comparison between these predicted values and experimental measurements will be made in Sec. IV. The growth rate of the instability ω_i was calculated for the case of an azimuthal current density $J_\theta = 1.1$ A cm^{-2} in order to satisfy the assumption of a tenuous electron ring, and is also indicated in Table I. In the actual experiments, the azimuthal current density is estimated to be ~ 60 A cm^{-2}. In the so-called "single particle, high-gain strong pump" regime[2] the instability growth rate is proportional to $J_\theta^{1/3}$, which implies that the experimental growth rates would be about a factor of 4 higher than those given in the table. The last column of Table I lists the estimated saturation efficiency η caused by phase trapping of electrons in the ponderomotive potential.

III. EXPERIMENTS

A. Apparatus

The general experimental configuration is shown in Fig. 1. A hollow, nonrotating electron beam is field emitted from a 6 cm radius, knife-edge cathode located 7.5 cm upstream of a brass anode plate. A 5 mm wide aperture slit in the anode plate allows a fraction of the electron beam current to pass through the anode plane into the cusp transition region. The cusp magnetic fields are produced by two independently controllable solenoids, and a soft iron plate is used to narrow the axial extent of the cusp transition region. The measured FWHM of the radial component of the magnetic field at the center of the cusp is 4 mm. The $\mathbf{v}_z \times \mathbf{B}_r$ force acts to convert axial electron velocity upstream of the cusp transition region into azimuthal velocity downstream, with resulting downstream beam parameters of 2 MeV, 1 kA, and 5

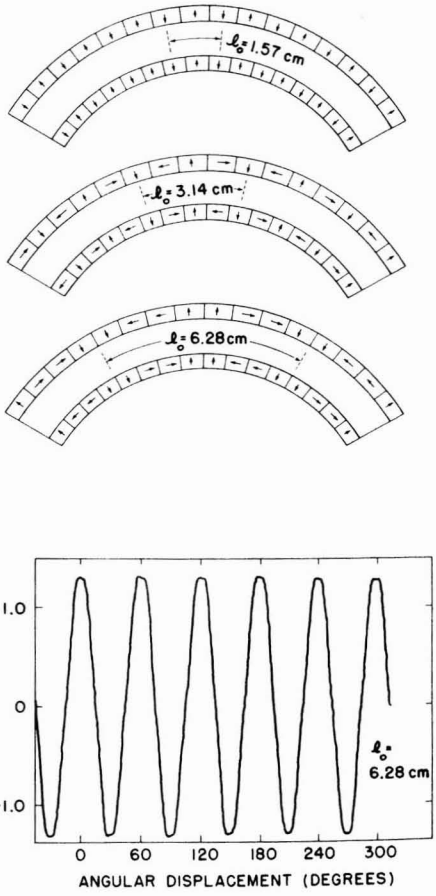

FIG. 3. Arrangment of bar magnets (top); Hall probe measurement of the wiggler field at a radial position $r = 5.92$ cm, as a function of azimutha angle (bottom).

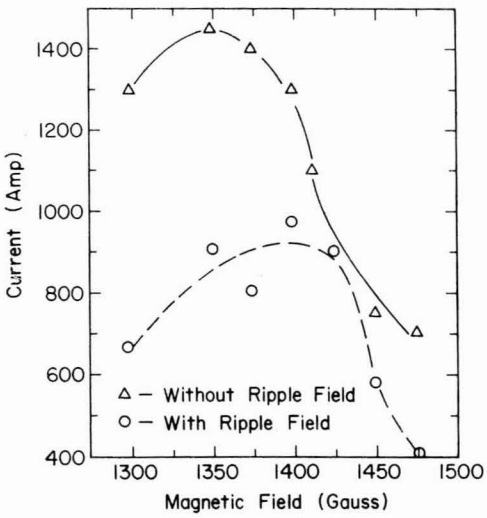

FIG. 4. Peak current exiting the interaction region versus applied cusp axial magnetic field. Results with and without the wiggler magnets are shown.

nsec. Because the cusp reflects all electrons with energies less than a threshold value given by

$$E_{\text{th}} = [(m_0c^2)^2 + (cer_cB)^2]^{1/2} - m_0c^2,$$

the total energy spread in the downstream rotating beam is in the range 1%–3%. The velocity spread caused by local temperature in the beam has been estimated to be about 0.2%.

The downstream beam rotates between two concentric stainless steel cylinders of radii 5.40 and 6.51 cm, respectively. Single turn Rogowski coils can be located at the upstream and/or downstream ends of the interaction region to measure the axial current entering or leaving the wiggler region with or without the wiggler magnets in place. The samarium cobalt magnets used to provide the wiggler field are placed behind the cylinders and held in place by grooved aluminum holders. Typical arrangements of the magnets to achieve various periodicities are shown in Fig. 3. The axial length of the wiggler field is about 20 cm, and the wiggler strength has been varied in the experiments by simply removing some of the magnets from the 6.28 cm wiggler configuration shown in the figure.

The radiation generated in the experiments is measured with a small horn antenna located immediately downstream of the interaction region. The radiated power spectra for various configurations has been measured using a sensitive grating spectrometer,[21] with gratings available in the range 70–200 GHz. The frequency resolution of the spectrometer is typically $\Delta f/f = 0.02$, and the insertion loss is in the range 3–5 dB.

B. Electron beam measurements

Measurement of the axial electron beam current exiting the interaction region with and without the wiggler magnets in place has been made using a single turn Rogowski coil located immediately downstream of the wiggler region. The results, shown in Fig. 4, indicate that a wiggler field of 1300

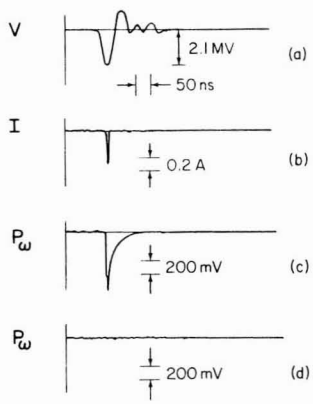

FIG. 5. Oscilloscope waveforms of (a) diode voltage, (b) axial current collected by a 2.24 mm^2 collector located in the center of the interaction region, (c) microwave signal in T band (91–170 GHz) with wiggler magnets, and (d) microwave signal in T band without wiggler magnets.

G amplitude and $l_0 = 6.28$ cm causes a drop in the beam current of only about 30%. These results confirm that the wiggler field does not have a disastrous effect on the electron orbits, a result consistent with the single particle orbit calculations. In fact, it is likely that the wiggler field acts to remove electrons with badly off-centered orbits from the beam.

Another indication of the nature of the beam current pulse shape has been obtained by placing a small-area axial current collector midway between the conducting cylinders at the axial center of the wiggler field region. A typical current pulse waveform is shown in Fig. 5 and shows dramatically the shortening of the downstream electron beam current pulse duration caused by the reflection of all low-energy electrons at the cusp transition region. This independent measurement of the beam current in the wiggler region also shows that even a relatively strong wiggler field does not disastrously disrupt the rotating electron beam.

C. Radiation measurements

Initial measurements of the radiation produced by the interaction of the rotating electron beam with the wiggler field involved inserting a small horn antenna into the region

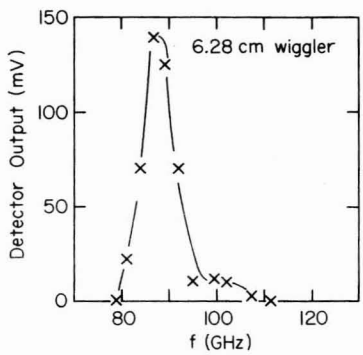

FIG. 6. Radiated power spectrum for $B_{0w} = 1300$ G, $l_0 = 6.28$ cm.

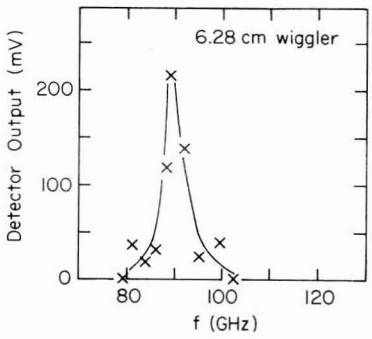

FIG. 7. Radiated power spectrum for $B_{0w} = 800$ G, $l_0 = 6.28$ cm.

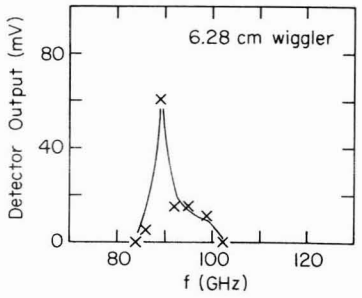

FIG. 9. Radiated power spectrum for $B_{0w} = 450$ G, $l_0 = 6.28$ cm, with inner magnets and inner conducting boundary removed.

immediately downstream of the interaction region and bringing the signal out through a length of Ka-band (22–40 GHz) waveguide. The radiation was then guided through various waveguide filters into calibrated attenuators and detectors. The receiving horn was oriented in such a way as to pick up TM waves in the coaxial conducting boundary system. In these initial experiments, a wiggler field amplitude of 1300 G and a wiggler period of 6.28 cm were used exclusively. Typical signals obtained in T band (91–170 GHz) with and without the wiggler magnets in place are shown in Fig. 5, and show dramatically that high-frequency radiation is only observed when the wiggler field is present. Because of the difficulty in efficiently coupling radiation out of the system, we have only been able to estimate the total radiated power as being in excess of 200 kW. Therefore, a reliable measurement of the electronic efficiency of the experiment is currently unavailable. These results have been reported previously.[15]

In these measurements, the horn has been located in various configurations, and the radiated power has been observed to be greatest in the direction of the electron orbits, as expected if the radiation is scattered in the forward direction as in a linear FEL. If the horn is moved to detect radiation in the opposite direction, the observed radiation is down by more than 10 dB. Waveguide cutoff filters were used to obtain a rough idea of the frequency content of the radiation. From these measurements it was determined that most of the radiated power was within N band (74–140 GHz).

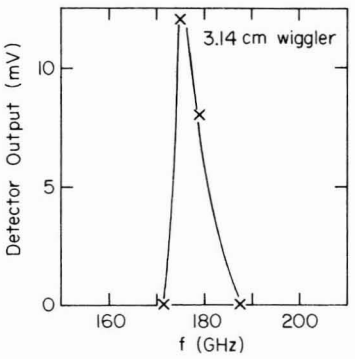

FIG. 8. Radiated power spectrum for $B_{0w} = 1000$ G, $l_0 = 3.14$ cm.

Detailed measurements of the radiation spectra have been obtained for a variety of wiggler configurations using the grating spectrometer described previously. These configurations include (a) the 1300 G, 6.28 cm period wiggler first studies (Fig. 3, bottom magnet array), (b) an 800 G, 6.28 cm wiggler (same array, every other magnet removed), (c) a 1000 G, 3.14 cm wiggler (middle magnet array), and (d) a 450 G, 6.28 cm wiggler in which the inner magnets and the inner conducting boundary were removed entirely. Plots of detector output versus frequency are shown for these configurations in Figs. 6–9, respectively.

Several features of these spectra are worthy of mention. First, the radiation observed in all cases is very narrow band, approaching the resolving power of the spectrometer. Second, the center frequency for the 3.14 cm wiggler (175 GHz) is almost exactly double that observed for the 6.28 cm wiggler (88 GHz), and both frequencies are in close agreement with the predictions of theory summarized in Table I. This last result may be just a chance occurrence, as the predictions of the theory are quite sensitive to the values chosen for the electron beam energy and the applied magnetic field.

Although the detector used for these measurements has a sensitivity that does not vary substantially over a frequency range of 10 GHz or so, the detector sensitivity does fall steadily as the frequency of the detected signal is increased. As a result of this trend and the fact that we do not have a calibration source at 175 GHz, even a comparative estimate of the power radiated at this frequency is not possible. If we extrapolate our calibration of the detector response versus frequency from our data in the range 26–135 GHz, where we do have calibration sources, then the radiated power at 175 GHz appears to be roughly comparable to that at 88 GHz.

IV. CONCLUSIONS

The experimental studies indicate that the production of millimeter wave radiation by the interaction of a rotating electron beam with an azimuthally periodic wiggler field has been achieved in a manner consistent with theoretical expectations. The agreement between the measured radiation frequencies and predicted values given in Table I is excellent, but further work will be need in order to determine if radiation is also produced at the other frequencies indicated. Although the efficiency of conversion of electron beam energy to radiation is currently low (less than 1%), it is not at all clear how efficiently the radiation is currently being coupled

ut of the system. In addition, no attempts have been made o minimize wall losses or to optimize the experimental conguration for maximum radiated power. For example, it nay be possible to design a system that will be unstable at nly one frequency, in contrast to the several unstable frequencies predicted for the present configuration.

We note that in order to achieve frequencies similar to hose reported above, the gyrotron[22] would require magnetic ields more that an order of magnitude higher. Comparing ω_i and η of Table I with those of a gyrotron operating with similar parameters, one finds that the gyrotron has somewhat lower growth rates ω_i, but higher efficiencies η.

Future studies of this novel source of coherent radiation will include attempts to generate submillimeter radiation by reducing the wiggler period and experiments using lower energy and lower current electron beams with longer pulse durations.

ACKNOWLEDGMENTS

It is a pleasure to acknowledge the assistance of A. Bromborsky in performing the orbit calculations.

This work was supported by the U. S. Department of Energy and the Air Force Office of Scientific Research.

[1]N. M. Kroll and W. A. McMullin, Phys. Rev. A **17,** 300 (1978); P. Sprangle and R. A. Smith, Phys. Rev. A **21,** 293 (1980) and references therein.
[2]P. A. Sprangle, R. A. Smith, and V. L. Granatstein, in *Infrared and Submillimeter Waves*, edited by K. Button (Academic, New York, 1979), Vol. 1, p. 279 and references therein.
[3]W. A. McMullin and G. Bekefi, Appl. Phys. Lett. **39,** 845 (1981).
[4]W. A. McMullin and G. Bekefi, Phys. Rev. A **25,** 1826 (1982).
[5]R. C. Davidson and W. A. McMullin, Phys. Rev. A **26,** 1997 (1982).
[6]R. C. Davidson and W. A. McMullin, Phys. Fluids **26,** 840 (1983).
[7]S. Benson, D. A. G. Deacon, J. N. Eckstein, J. M. J. Madey, K. Robinson, T. I. Smith, and R. Taber, J. Phys. (Paris) Colloq. **44,** C1-353 (1983).
[8]M. Billardon, P. Elleaume, J. M. Ortega, C. Bazin, M. Bergher, M. Velghe, Y. Petroff, D. A. G. Deacon, K. E. Robinson, and J. M. J. Madey, Phys. Rev. Lett. **51,** 1652 (1983).
[9]J. A. Edighoffer, G. R. Niel, C. E. Hess, T. I. Smith, S. W. Fornaca, and H. A. Schwettman, Phys. Rev. Lett. **52,** 344 (1984).
[10]T. J. Orzekhowski, B. Anderson, W. M. Fawley, D. Prosnitz, E. T. Scharlemann, S. Yarema, D. Hopkins, A. C. Paul, A. M. Sessler, and J. Wurtele, submitted to Phys. Rev. Lett.
[11]G. Bekefi, Appl. Phys. Lett. **40,** 578 (1972).
[12]R. C. Davidson, W. A. McMullin, and K. Tsang, Phys. Fluids **27,** 233 (1984).
[13]C-L. Chang. E. Ott, T. M. Antonsen, Jr., and A. T. Drobot, Phys. Fluids **27,** 2937 (1984).
[14]G. Bekefi, R. E. Shefer, and B. D. Nevins, *Proceedings of the International Conference on Lasers '82,* New Orleans, Louisana, December 1982, edited by R. C. Powell (STS Press, McLean, Virginia, 1982), p. 136.
[15]G. Bekefi, R. E. Shefer, and W. W. Destler, Appl. Phys. Lett. **44,** 280 (1984).
[16]Y. Z. Yin and G. Bekefi, Phys. Fluids **28,** 1186 (1985).
[17]M. J. Rhee and W. W. Destler, Phys. Fluids **17,** 1574 (1974).
[18]W. W. Destler, H. Romero, C. D. Striffler, R. L. Weiler, and W. Namkung, J. Appl. Phys. **52,** 2740 (1981).
[19]W. W. Destler, R. L. Weiler, and C. D. Striffler, Appl. Phys. Lett. **38,** 570 (1981).
[20]P. Sprangle, J. Appl. Phys. **47,** 2935 (1976).
[21]J. Fischer, D. A. Boyd, A. Cavallo, and J. Benson, Rev. Sci. Instrum. **54,** 1085 (1983).
[22]P. Sprangle and A. T. Drobot, IEEE Trans. Microwave Theory Tech. **MTT-25,** 528 (1977).